Cytochrome P450 2E1 null mice provide novel protection against cisplatin-induced nephrotoxicity and apoptosis

Hua Liu and Radhakrishna Baliga

Department of Pediatrics, University of Mississippi Medical Center, Jackson, Mississippi

Cytochrome P450 2E1 null mice provide novel protection against cisplatin-induced nephrotoxicity and apoptosis.

Background. Reactive oxygen metabolites (ROM) are important mediators of cisplatin-induced nephrotoxicity and apoptosis. The site and source of generation of these metabolites are not well defined. Cytochrome P450 (CYP) are heme-containing enzymes that can generate ROM during the oxidative metabolism of exogenous and endogenous compounds. CYP2E1 was identified and localized to the kidney proximal tubule. There is evidence to suggest that CYP2E1 is involved in the generation of ROM.

Methods. The current study was performed utilizing CYP2e1 null mice (*CYP2e1−/−*). Cisplatin nephrotoxicity was induced in mice by single intraperitoneal injection of cisplatin and animals were sacrificed 72 hours later. Renal function was assessed and various biochemical tests were performed, including histologic studies.

Results. *CYP2e1−/−* demonstrated marked functional and histologic protection against cisplatin-induced renal injury. Incubation of *CYP2e1−/−* kidney slices with cisplatin resulted in significant decrease in the generation of ROM and attenuation of cytotoxicity as compared to that of wild-type mice (*CYP2e1+/+*). Cisplatin-induced apoptosis was also markedly reduced in the *CYP2e1−/−* mice. Direct incubation of cisplatin with the microsomes isolated from *CYP2e1−/−* kidney cortex produced significant decrease in the generation of hydrogen peroxide, catalytic iron content, and hydroxyl radical formation compared to *CYP2e1+/+* microsomes.

Conclusion. Our results thus demonstrate a pivotal role of CYP2E1 in cisplatin-induced nephrotoxicity and apoptosis. We postulate that the interaction of cisplatin with CYP2E1 results in the generation of ROM that causes renal injury and initiates apoptosis.

Cisplatin is one of the most effective chemotherapeutic agents used in the treatment of a variety of human solid tumors [1]. The most common adverse effect limiting the use of cisplatin is the nephrotoxicity that devel-ops primarily in the S_3 segment of the proximal tubule [2, 3]. Reactive oxygen metabolites (ROM) have been implicated to play an important role in cisplatin-induced renal cell injury [4–7]. There is little information as to the intracellular source and site for the generation of ROM in this model.

Cytochrome P450 (CYP) is a group of hemeproteins that act primarily as mono-oxygenases in the synthesis and metabolism of many exogenous and endogenous compounds [8]. During the nicotinamide adenine dinucleotide phosphate (NADPH)-dependent electron transfer CYP can function as oxidases and generate hydrogen peroxide (H_2O_2) and superoxide anion [9, 10]. These initial ROM may oxidatively degrade the CYP hemeprotein and promote the release of iron leading to the generation of the potent oxidants. Recent studies, including ours, indicate that the iron rich enzyme, CYP, may serve as an important source of catalytic iron in models of tissue injury, including cisplatin nephrotoxicity [11–15].

CYP2E1 is clinically and toxicologically important and is constitutively expressed in the liver and many other tissues, including the kidney [16]. This enzyme is also up-regulated in certain pathophysiologic conditions such as diabetes [17], starvation [18], and obesity [19]. CYP2E1 exhibits a unique ability to potentiate an iron catalyzed Fenton-type reaction and an increased rate of microsomal lipid peroxidation [20, 21]. We have identified and localized CYP2E1 to the proximal tubule of the mouse kidney. A *CYP2e1* null mouse (*CYP2e1−/−*) line has been established with no phenotypic or pathologic abnormalities indicating that CYP2E1 is not essential for the normal mammalian development or physiologic homeostasis [22]. When challenged with cisplatin, the *CYP2e1−/−* mice provided marked functional and histologic protection against cisplatin-induced nephrotoxicity and apoptosis. Our results thus indicate an important role of CYP2E1 in cisplatin-induced renal cell injury and initiation of apoptosis.

We also looked at the induction of heme oxygenase (HO-1), which is a rate-limiting enzyme for heme metabolism that can be up-regulated in response to an increase

---

in heme and iron. p21, a cyclin kinase inhibitor, which has been shown to prevent DNA-damaged cells from entering the cell cycle, was also examined [23].

METHODS

CYP2e1 knockout mice

Mice (strain 129/SV) carrying a deletion of *CYP2e1* gene have been successfully produced in the laboratory of Dr. Gonzalez at the National Institutes of Health. The *CYP2e1* gene was isolated from a 129/SV mouse (CYP2E1 wild-type mouse, *CYP2e1*+/+) genomic library that contained the complete coding region. The gene was disrupted by the replacement of exon 2 with the PGK-NEO cassette [22]. Mice homozygous for the disrupted *CYP2e1* allele were born and developed normally with no obvious phenotypic divergence from wild-type mice. The clone of mice was maintained by breeding *CYP2e1*−/− males with *CYP2e1*−/− females. A complete absence of CYP2E1 protein and mRNA in the mice was confirmed by immunoblotting and Northern blot. The *CYP2e1* knockout mice provide us with a novel toxicologic model that enables the determination of the precise contribution of the particular CYP2E1 isozyme toward cisplatin-induced acute renal failure (ARF).

Cisplatin-induced ARF

Cisplatin model of ARF was induced in mice by single intraperitoneal injection of cisplatin at a dose of 10 mg/kg body weight as determined by a dose-dependent pilot study in our laboratory (data not shown). Male *CYP2e1*−/− and *CYP2e1*+/+ mice weighing 25 to 30 g were allowed free access to rodent chow (Purina) and water. The animals were sacrificed at 72 hours after cisplatin injection. Renal function was assessed by blood urea nitrogen (BUN), serum creatinine, creatinine clearance, and kidney histology.

Kidney histology

Three to five mice in each group were obtained for kidney histology. Renal function in these subsets was not different from the overall experimental groups. Renal tubule histologic grading was as follows: 0, normal; I, area of tubular epithelial cell swelling, vacuolar degeneration, necrosis, and desquamation involving <25% of cortical tubules; II, similar changes involving >25% but <50%; III, similar changes involving >50% but <75% tubules; IV, similar changes involving >75%.

Bleomycin-detectable iron assay

Iron capable of catalyzing free radical reactions was measured by bleomycin-detectable iron assay as described by Gutteridge, Rowley, and Halliwell [24, 25] and as detailed in our previous studies [4, 11, 12, 26].

Preparation of microsome fraction

Kidney cortex was suspended in an extraction buffer containing 20 mmol/L Tris-HCl, pH 7.4, 0.25 mol/L sucrose, 1 mmol/L ethylenediaminetetraacetic acid (EDTA) and protease inhibitor cocktail (25 mg protein/1 μL of cocktail, Sigma Chemical Co., St. Louis, MO, USA) and frozen at −80°C. Subsequently, the glomeruli were thawed and sonicated [27]. The homogenate was centrifuged at 15,000*g* for 20 minutes at 4°C. The supernatant obtained was again centrifuged at 105,000*g* for 60 minutes at 4°C. The sedimented microsomal pellet was resuspended in above extraction buffer to give a protein concentration ~10 mg/mL [28].

Western blot analysis

The microsome fraction obtained was subjected to sodium dodecyl sulfate-polyacrylamide gel electrophoresis (SDS-PAGE) in 1 mm slab gels. The separated forms were transferred from the gel to a nitrocellulose sheet using a Mini Trans-Blot electroblotting unit (Bio-Rad, Hercules, CA, USA). The primary antibodies were anti-CYP2E1 (MFO 100, StressGen, Victoria, BC, Canada), anti-HO-1 (SPA 895, StressGen, Victoria, BC, Canada), and monoclonal anti-p21 (sc-6246, Santa Cruz Biotechnology, Inc., Santa Cruz, CA, USA). Subsequent to primary and secondary antibody (peroxidase-labeled) treatment, the blots were visualized by enhanced chemiluminescence method [29].

Immunohistochemistry

Kidney cortical sections were fixed in 10% buffered formalin for 6 hours and embedded in paraffin. After deparaffinization and antigen retrieval, the sections were immunolabeled and visualized according to an avidin-biotin complex (ABC) method [30].

Immunoelectronmicroscopy

Kidney cortical sections were fixed in 4% paraformaldehyde, postfixed in osmium tetraoxide, dehydrated and embedded in LR-White resin. Semithin sections were cut to ensure that the sections contained glomeruli, then 70 nm ultrathin sections were cut from selected blocks and placed on nickel grids. Grids were incubated with normal goat serum for 30 minutes, then placed in monoclonal anti-CYP2E1 antibody for overnight at 4°C. Grids were rinsed in Tris buffer and then incubated in antirabbit immunoglobulin G (IgG) antibody (BB International, Cardiff, UK, 1:100 dilution) conjugated with 10 nm gold for 1 hour at room temperature. Grids were rinsed in buffer, dried, and viewed with a Leo 906 transmission electron microscope.

Reverse transcription-polymerase chain reaction (RT-PCR)

RNA was isolated from the kidney cortex using TRIzol Reagent (GibcoBRL, Gaithersburg, MD, USA). RT of
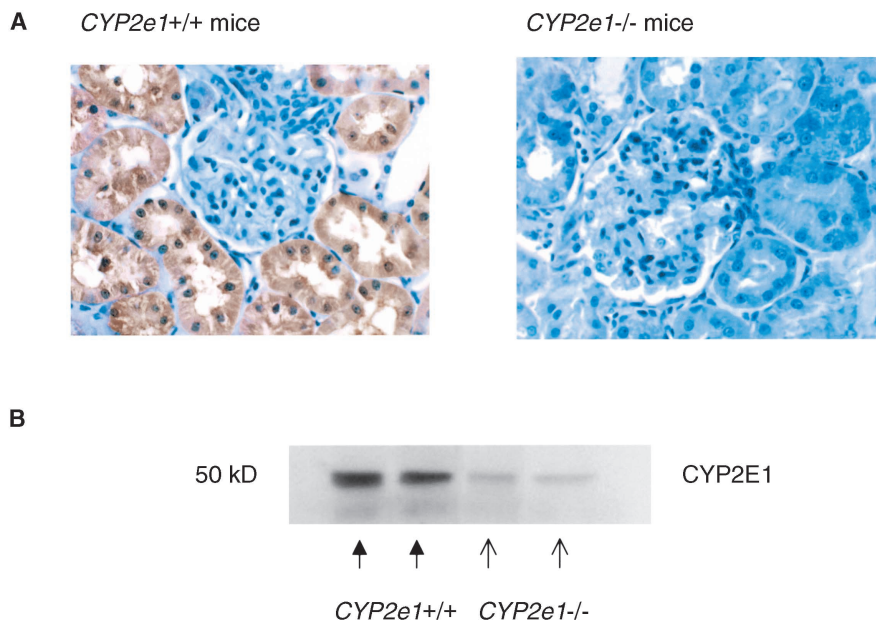
A   *CYP2e1+/+ mice*   *CYP2e1-/- mice*

B

Fig. 1. **Characterization of *CYP2e1 −/−* mice by immunohistochemistry (*A*) and Western blot (*B*).** Western blot detection of *CYP2E1* was performed by using the microsome isolated from liver. *CYP2E1* is expressed in *CYP2e1 +/+* mice both in liver and kidney proximal tubules but not in *CYP2e1 −/−* mice.

0.5 µg of total RNA and PCR were carried out by one-step RT-PCR protocol using AccessQuick RT-PCR system (Promega, Madison, WI, USA). p21 primers described by Gartel et al [31] were purchased from Gibco BRL. The sense primer was 5′-AGCCTGAAGACTGT GAT GGG-3′, and the antisense 5′-AAAGTTCCAC CGT TCTCGG-3′. The amplification product length was 228 bp. GAPDH sense was 5′-TCCCTCAAGATTG TCAGCAA-3′; and GAPDH antisense 5′-AGATCC ACAAC GGATACATT-3′. The amplification conditions for PCR were a hot start of 95°C for 50 seconds, followed by cycling of 1 minute at 60°C, 1 minute at 72°C, and 1 minute at 95°C for 30 cycles. The reaction was finished within 7 minutes at 72°C. The PCR products were visualized on a 2% agarose gel using ethidium bromide and ultraviolet transillumination.

Preparation of renal cortical slices and incubation condition

Renal cortical slices were prepared as described by Zhang and Lindup [32]. Male *CYP2e1 −/−* and *CYP2e1 +/+* mice weighing 25 to 30 g were anesthetized and the kidneys were purfused with ice-cold saline to remove as much blood as possible. After removing the kidneys, renal cortical slices were prepared using a McILWAIN Tissue Chopper (Surrey, England). The slices (six to eight slices, 0.3 to 0.5 mm thick, weight 80 to100 mg) were incubated with oxygenated medium (97 mmol/L NaCl, 40 mmol/L KCl, 0.74 mmol/L $CaCl_2$, 1 mmol/L glycine, 1 mmol/L glutamate, 0.2 mmol/L L-cysteine, and 7.5 mmol/L sodium phosphate buffer, pH 7.4) in presence or absence of cisplatin at 37°C. The dose of cisplatin utilized was based on a time- and dose-dependent study of cisplatin cytotoxicity (data not shown).
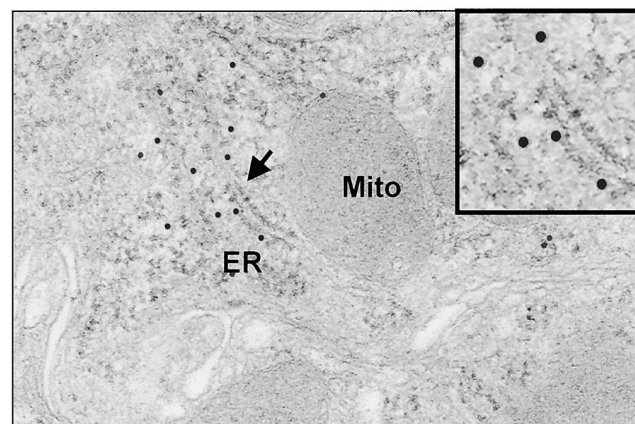

Fig. 2. **Immunoelectronmicroscopy for CYP2E1 revealed gold particles located primarily at the endoplasmic reticulum.** Magnification ×90,000.

Measurement of intracellular H_2O_2 generation from kidney slices

The principle of this method is that the oxidation of 2′,7′-dichlorofluorescin-diacetate (DCFH-DA) in the presence of H_2O_2 produces the highly fluorescent compound 2′,7′-dichlorofluorescin (DCF), which can be measured by a fluorometer. The intracellular generation of H_2O_2 in kidney slices was tested by a microplate assay described by Rosenkranz et al [33]. In brief, kidney slices were incubated at 37°C with equal volumes of DCFH-DA (10 uL/mL) and cisplatin for the planned time period. At the end of the incubation, the fluorescence intensity was read using a fluorescence spectrophotometer (wavelength 485/535 nm) capable of reading microtiter plates.

Table 1. Renal function and catalytic iron

	Blood urea nitrogen mg/dL	Serum creatinine mg/dL	Creatinine clearance mL/hour	Catalytic iron nmol/mg protein
CYP2e1+/+				
Sham (N = 6 to 9)	17 ± 2	0.27 ± 0.02	7.21 ± 0.9	11.47 ± 0.18
Cisplatin (N = 8 to 14)	69 ± 2[a]	1.55 ± 0.23[a]	1.02 ± 0.2[a]	38.98 ± 3.88[a]
CYP2e1−/−				
Sham (N = 6)	15 ± 3	0.27 ± 0.02	7.71 ± 0.5	6.54 ± 0.96
Cisplatin (N = 10)	32 ± 4[a,b]	0.47 ± 0.06[b]	6.24 ± 0.8[b]	12.08 ± 1.33[b]

Values are mean ± SE. [a]$P < 0.05$ compared to the respective control, [b]$P < 0.05$ compared to *CYP2E1+/+* mice treated with cisplatin. There is no significant difference in the control values between *CYP2e1+/+* and *CYP2e1−/−*.
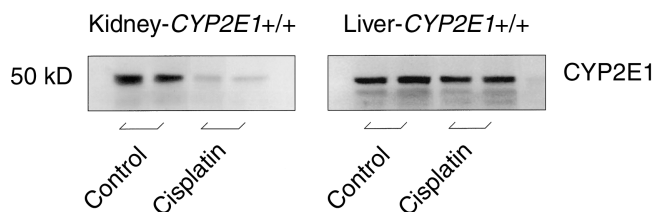

Fig. 3. The effect of cisplatin on CYP2E1 content in renal cortex and liver of *CYP2e1+/+* mice as evaluated by Western blot. The loss of CYP2E1 content in the renal cortex is injury specific since there was no difference in the level of CYP2E1 content in the liver between the untreated and the cisplatin-treated animals.

Measurement of hydroxyl radical formation from kidney slices

2-deoxy-D-ribose in a final concentration of 3 mmol/L was added to the medium just prior to the incubation. At the end of the incubation, the incubation medium was collected for the measurement of hydroxyl radical formation by deoxyribose degradation method as in our previous study [34].

Detection of DNA fragmentation

The kidney cortex was homogenized and lysed with a buffer containing 10 mmol/L Tris-HCl (pH7.5), 1 mmol/L EDTA, 0.1 mmol/L NaCl, and 0.5% SDS. The lysates were incubated with proteinase K (0.2 mg/mL) at 50°C overnight. DNA was isolated from the lysates following the procedures as described by Ramachandra and Studzinski [35]. The DNA obtained was resuspended in a buffer (10 mmol/L Tris-HCl and 1 mmol/L EDTA) at 1 μg/mL and incubated with 0.1 U/10 μg DNA of DNAase free RNAase cocktail (Cat # 2286, Ambion, Austin, TX, USA). Electrophoresis was performed in 1.6% agarose gels and DNA was visualized with ethidium bromide.

Terminal deoxynucleotidyl transferase-mediated uridine triphosphate nick end labeling (TUNEL) staining

Detection of apoptotic cells in the kidney was performed on paraffin embedded renal tissue section utilizing a detecting kit, ApopTag Plus (Cat #S7101, Intergen, Purchase, NY, USA), following the manufacturer's protocol.

Statistical analysis

Values are expressed as mean ± standard error (SE). Statistical analysis was performed using unpaired t test (for only two groups) and analysis of variance (for more than two groups). Statistical significance was considered at $P < 0.05$.

RESULTS

CYP2E1 was identified and localized to the renal tubules but not the glomeruli (Fig. 1A). Analysis pertaining to the expression of CYP2E1 in the genetically altered mice (*CYP2e1−/−*) and wild-type mice (*CYP2e1+/+*) are summarized in Figure 1.

Ultrastructural localization by immunogold labeling indicated that CYP2E1 is predominantly present in the endoplasmic reticulum (Fig. 2).

The renal function as measured by the BUN, serum creatinine, and creatinine clearance is shown in Table 1. On day 3 following cisplatin injection *CYP2e1−/−* mice demonstrated significant preservation of renal function as compared to *CYP2e1+/+* mice.

Catalytic iron content was markedly increased in the kidneys of cisplatin-treated *CYP2e1+/+* mice (Table 1) associated with a marked decrease in the CYP2E1 content as determined by Western blot (Fig. 3) and immuno-histochemistry (Fig. 4). The loss of CYP2E1 content in the kidneys of the *CYP2e1+/+* mice was injury specific as there was no difference in the level of the CYP2E1 content in the liver between the untreated and cisplatin-treated mice (Fig. 3). The catalytic iron content was significantly reduced in the kidneys of the *CYP2e1−/−* mice injected with cisplatin (Table 1).

The histologic changes were graded as described in the **Methods** section and summarized in Table 2.

Cisplatin-treated *CYP2e1+/+* mice had extensive epithelial cell vacuolization, swelling, desquamation, and necrosis (grade 4) occurring predominantly in the proximal convoluted tubules (Fig. 5). There were very few changes observed in the *CYP2e1−/−* mice treated with cisplatin (grades 0 to 1) (Fig. 5).

Oxidant stress induces HO-1, the rate-limiting enzyme in heme degradation, which has been shown to be protec-
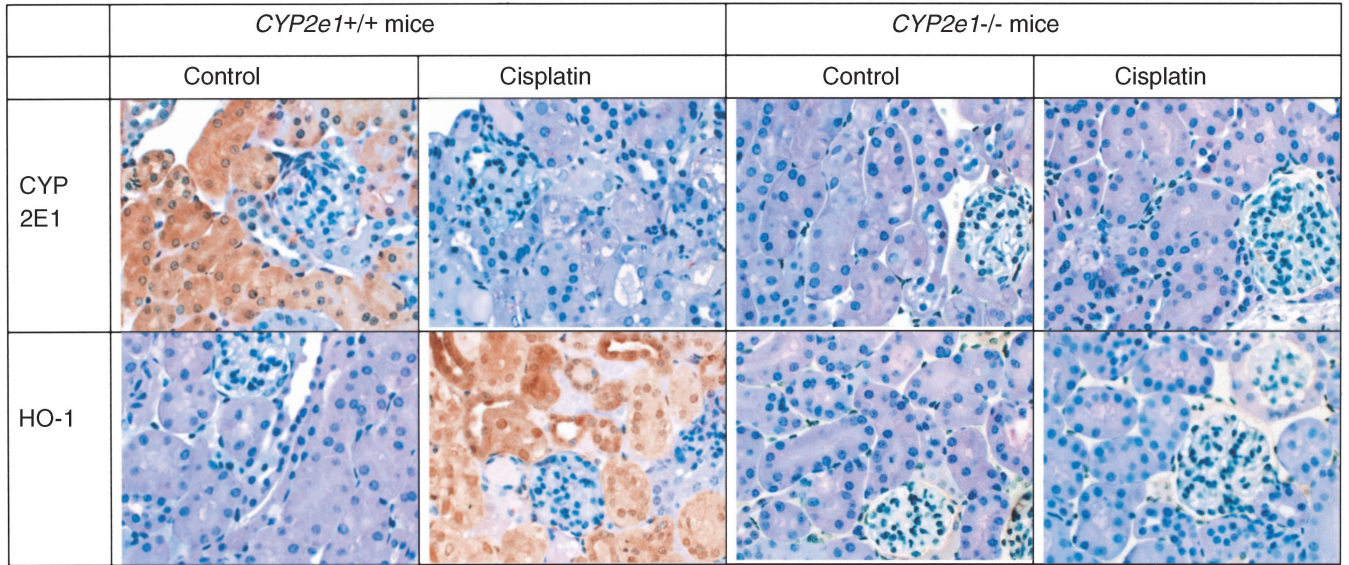
Fig. 4. Immunohistochemistry studies of the effect of cisplatin on CYP2E1 content and HO-1 induction in mouse renal cortex. The first row shows representative photographs using primary antibodies to CYP2E1, in animals injected with saline versus animals injected with cisplatin. The second row shows the same animals studied with primary antibodies to HO-1.
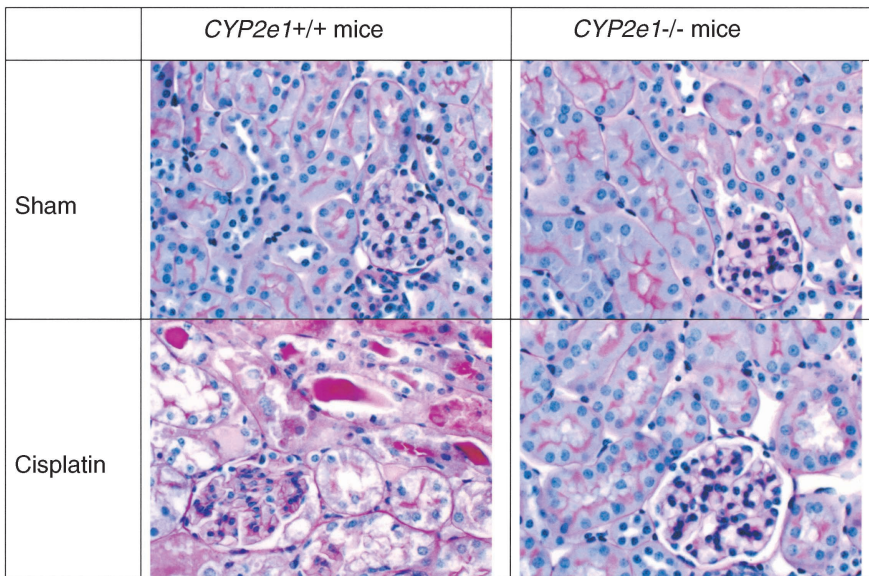

Fig. 5. Light-microscopy section of kidney. The first row shows representative photographs of the kidney sections from normal *CYP2e1+/+* and *CYP2e1−/−* mice. The second row shows the kidney sections from the mice treated with cisplatin. Cisplatin-treated *CYP2e1+/+* mice, but not *CYP2e1−/−* mice, had extensive epithelial cell vacuolization, swelling, desquamation, and necrosis predominantly in the proximal tubules.

Table 2. Histologic grading

| | | Histologic grade | | | | |
Group	N	0	I	II	III	IV
CYP2e1+/+ mice						
Control	3	3				
Cisplatin	5				1	4
CYP2e1−/− mice						
Control	3	3				
Cisplatin	5	3	2			

Three to five mice in each group were obtained for kidney histology. Renal function in these subsets was not different from the overall experimental groups. Renal tubule histologic grading was as follows: 0, normal; I, area of tubular epithelial cell swelling, vacuolar degeneration, necrosis, and desquamation involving <25% of cortical tubules; II, similar changes involving >25% but <50%; III, similar changes involving >50% but <75% tubules; IV, similar changes involving >75%.
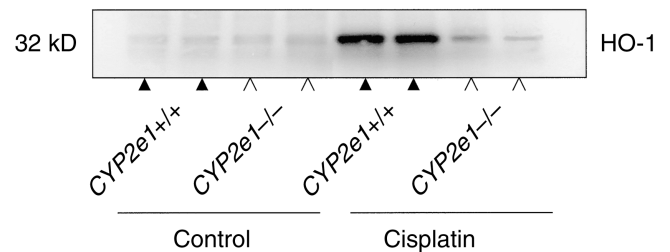

Fig. 6. Western blot analysis of HO-1 induction in renal cortex of *CYP2e1+/+* and *CYP2e1−/−* mice treated with 10 mg/kg intraperitoneal injection of cisplatin.

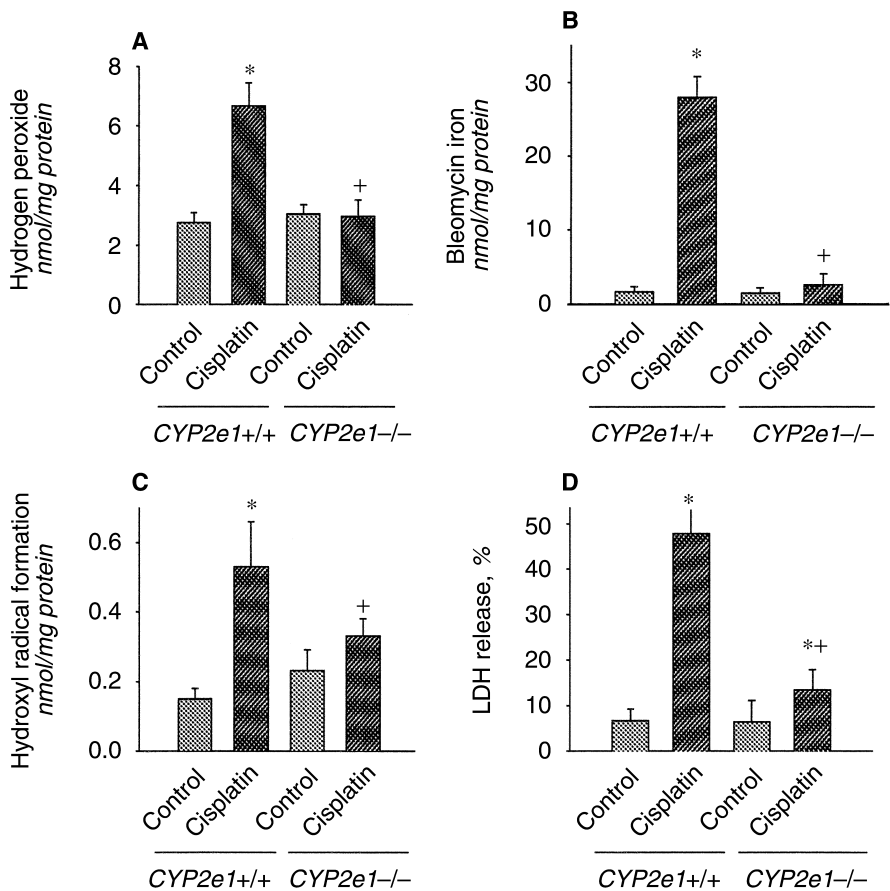Fig. 7. **In vitro study using kidney slices from**
CYP2e1 +/+ and CYP2e1 −/− mice. Hydrogen peroxide generation (*A*), catalytic iron release (*B*) and hydroxyl radical formation (*C*) from the kidney slices exposed to cisplatin (2 mmol/L for 1 hour at 37°C). Cytotoxicity of cisplatin (2 mmol/L for 2 hours at 37°C) to the kidney slices as measured by lactate dehydrogenase (LDH) release (*D*). Values are means ± SE, *N* = 4. *$P < 0.05$ compared to the respective control; +$P < 0.05$ compared to the *CYP2e1 +/+* kidney slices treated with cisplatin alone.

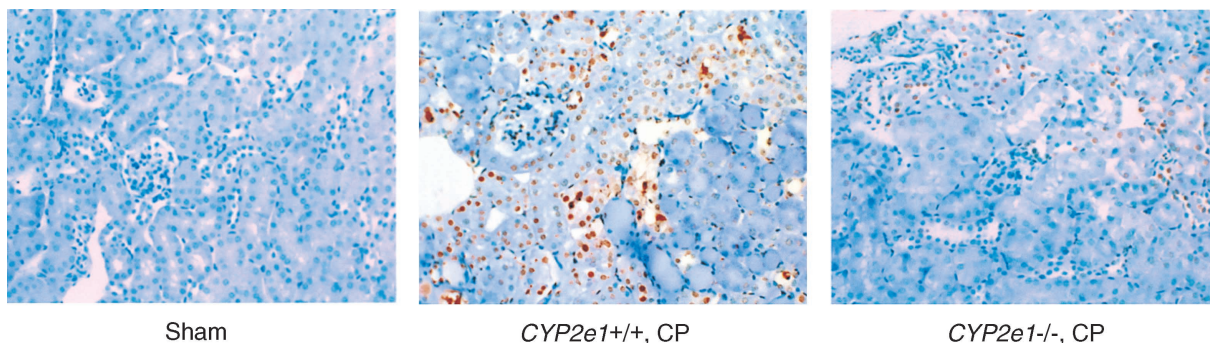Sham   *CYP2e1+/+, CP*   *CYP2e1-/-, CP*

Fig. 8. **Representative sections of terminal deoxynucleotidyl transferase-mediated uridine triphosphate nick end labeling (TUNEL) staining for detection of apoptotic nuclei in kidney cortex 72 hours after cisplatin injection.** TUNEL-positive cells were observed in the kidney of the *CYP2e1 +/+* mice treated with cisplatin but absent in control mice and markedly reduced in *CYP2e1 −/−* mice treated with cisplatin.

tive in several models of nephrotoxic renal injury [36]. Administration of cisplatin to *CYP2e1 +/+* mice resulted in marked induction of HO-1 in the tubules as demonstrated by immunohistochemistry (Fig. 4) and Western blot (Fig. 6). The induction of HO-1 was significantly attenuated in the *CYP2e1 −/−* mice.

The role of CYP2E1 was also examined in an in vitro model of cisplatin-induced toxicity to kidney slices. Exposure of *CYP2e1 +/+* kidney slices to cisplatin led to a

significant increase in the H_2O_2 generation (Fig. 7A), increase in the catalytic iron content (Fig. 7B) and hydroxyl radical formation (Fig. 7C). This was significantly reduced when *CYP2e1 −/−* kidney slices were incubated with cisplatin (Fig. 7 A to C). *CYP2e1 −/−* kidney slices markedly reduced cisplatin-induced cytotoxicity as measured by the lactate dehydrogenase (LDH) release (Fig. 7D).

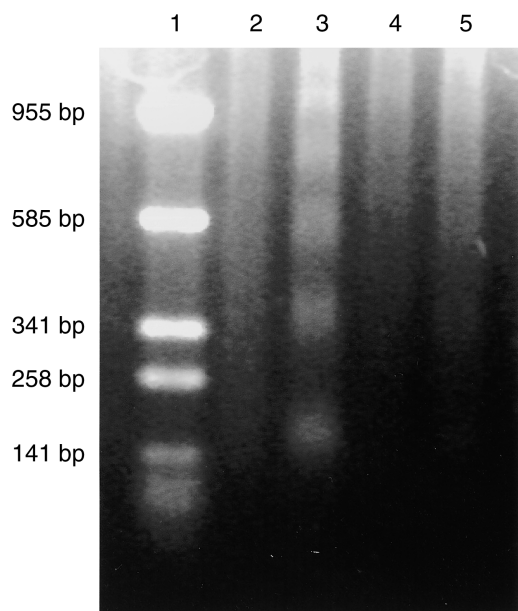Apoptotic bodies were noted in the hematoxylin and eosin–stained kidney sections in the *CYP2e1 +/+* mice

Fig. 9. Agarose gel electrophoresis of DNA from kidney cortex of *CYP2e1+/+* and *CYP2e1−/−* mice with and without cisplatin treatment. Column 1 is an oligonucleotide standard marker. Columns 2 and 4 are loaded with DNA from control mice of *CYP2e1+/+* and *CYP2e1−/−*, respectively. Columns 3 and 5 are from cisplatin-treated *CYP2e1+/+* and *CYP2e1−/−* mice, respectively. Apoptotic DNA fragments were induced in *CYP2e1+/+* (column 3) but not in other groups.

Fig. 10. The induction of p21mRNA and p21 protein in the kidney of *CYP2e1+/+* and *CYP2e1−/−* mice treated with cisplatin. Agarose gel (2%) electrophoresis of reverse transcription-polymerase chain reaction (RT-PCR) products of p21 mRNA and glyceraldehyde-3-phosphate dehydrogenase (GAPDH) mRNA (amplified at the same time for the internal standard) are presented as indicated. Western blot was performed by using a monoclonal anti-p21 antibody. Both p21 mRNA and p21 protein were up-regulated in cisplatin-treated mice as compared to respective control.

3 days after cisplatin injection. Exact quantification was not possible because of the extensive necrosis present in the kidney sections. To quantify the degree of apoptosis TUNEL assay was performed. Using this assay few stained nuclei were noted in the kidney sections of the control mice (Fig. 8). In the cysplatin-treated *CYP2e1+/+* mice a significant increase in the apoptotic cells was observed both in the proximal and distal regions of the nephron when compared to *CYP2e1−/−* mice (Fig. 8). DNA fragmentation as evidenced by the characteristic 180 bp laddering was attenuated in the cisplatin-treated *CYP2e1−/−* mice (Fig. 9).

In view of the importance of the cell cycle as a determinant of the fate of the cells, we examined the effect of cisplatin on the cell cycle protein p21. Both RT-PCR and Western analysis indicated a significant up-regulation of p21 in the *CYP2e1+/+* mice injected with cisplatin. Of interest was the induction of p21 in the *CYP2e1−/−* control mice with further up-regulation following administration of cisplatin (Fig. 10).

Direct incubation of the microsomes isolated from the *CYP2e1+/+* kidney with cisplatin resulted in a marked increase in the H_2O_2 and catalytic iron release with significant hydroxyl radical formation. This was attenuated when microsomes isolated from the *CYP2e1−/−* kidney were exposed to cisplatin (Fig. 11).
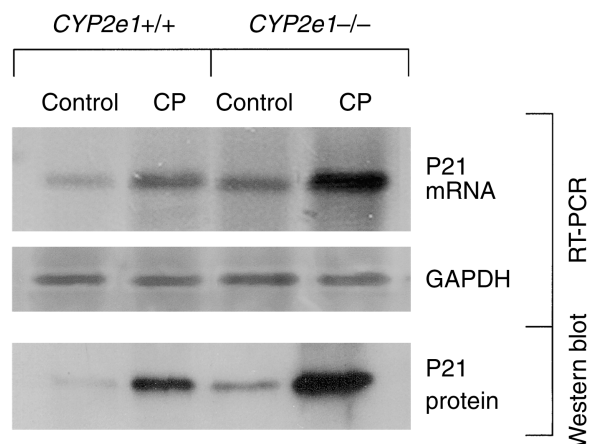
DISCUSSION

The importance of CYP in the pathologic process of the kidney seems to be increasing [37–39]. Its role as a site for ROM generation and a source of catalytic iron in the kidney has not been fully explored. We have recently demonstrated that exposure of LLC-PK1 cells (renal proximal tubular cells) to cisplatin resulted in marked generation of H_2O_2, loss of CYP2E1 content, increase in catalytic iron and hydroxyl radical formation accompanied by significant cytotoxicity. Treatment with CYP2E1 inhibitors markedly reduced H_2O_2 generation with the preservation of CYP2E1 content. There was also a marked decrease in catalytic iron and hydroxyl radical formation with significant attenuation of cytotoxicity [40].

In the current study, administration of cisplatin to *CYP2e1+/+* mice resulted in marked reduction of CYP2E1 content associated with a significant increase in catalytic iron. *CYP2e1−/−* mice prevented the catalytic iron formation and provided marked functional and histologic protection following cisplatin injection. Incubation of the kidney slices from *CYP2e1+/+* mice with cisplatin resulted in a marked generation of H_2O_2, catalytic iron and hydroxyl radical along with significant cytotoxicity. These effects of cisplatin were significantly reduced in *CYP2e1−/−* kidney slices. Similar results were observed on incubating the microsomes isolated from kidney of *CYP2e1+/+* and *CYP2e1−/−* mice with cisplatin. Taken together our data strongly suggest that CYP2E1 plays an important role in cisplatin-induced nephrotoxicity by serving as a major site for the generation of ROM and a significant source of iron capable of
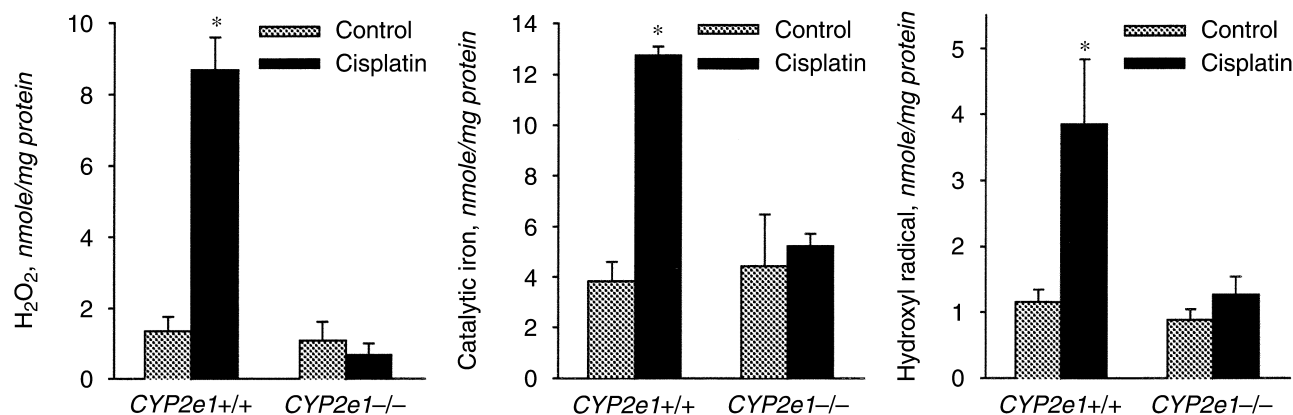
Fig. 11. Hydrogen peroxide generation (A), catalytic iron release (B), and hydroxyl radical formation (C) from the microsomes isolated from the kidney cortex of *CYP2e1*+/+ and *CYP2e1*−/− mice 60 minutes following cisplatin (200 μg/mL) treatment. Values are mean ± SE, $N = 4$. *$P < 0.05$, compared to respective controls.

catalyzing free radical reactions. We postulate that the interaction between cisplatin and CYP2E1 results in the generation of H_2O_2 that causes destruction of the heme protein with the release of heme and iron. The released iron then participates in the generation of the hydroxyl radical and other pathogenic oxidants resulting in injury.

Induction of HO-1 has been shown to be protective in nephrotoxic models of renal injury [41, 42]. Recent studies provide further genetic evidence that up-regulation of HO-1 serves as an important adaptive mechanism in the protection of cells against oxidative injury [43, 44]. Bissell and Hammaker [45] based on their study with endotoxin indicated that agents which promote the induction of HO-1 cause the release of heme from the CYP, which, in turn, causes the stimulation of HO-1. In the present study we have demonstrated that administration of cisplatin to the *CYP2e1*+/+ mice resulted in significant loss of CYP2E1 content in the kidney accompanied by an increase in the catalytic iron and significant induction of the HO-1 in the tubules. This up-regulation of HO-1 was markedly reduced in the cisplatin-treated *CYP2e1*−/− mice.

ROM plays an important role in cisplatin-induced apoptosis of the renal tubular cells [46]. Recent studies indicate that mitochondria are the principal sensors and thus critical in the initiation of the apoptotic cascade [47–49]. However, little is known about what triggers apoptosis in response to cisplatin. The prevailing assumption is that all electron-transfer processes leading to ROM production are localized to the mitochondria [50, 51]. However, consideration needs to be given to yet another electron-transfer chain namely the microsomes via the CYP system, which is crucial to the ROM-mediated cell signaling and is present at high concentration in the endoplasmic reticulum of most animal cells [52, 53]. Administration of cisplatin to *CYP2e1*−/− mice resulted in significant attenuation of apoptosis that was evident in the *CYP2e1*+/+ mice.

The p21 protein, an inhibitor of cyclin-dependent kinase, is found in the nucleus of most quiescent cells at low levels [54]. It is induced to high levels by oxidative stress and DNA damage effectively inhibiting the cell cycle progression [23, 55]. By utilizing *p21*−/− mice, Megyesi, Safirstein, and Price [56] have shown that p21 protects the cisplatin-induced kidney damage by preventing the DNA damaged cells from entering the cell cycle, which would otherwise result in death from apoptosis or necrosis. Inguaggiato et al have further demonstrated that the mechanisms by which induction of HO-1 protects against cisplatin-induced nephrotoxicity involves the p21 dependent mechanisms [44]. In the current study both RT-PCR and Western analysis indicated a significant up-regulation of P21 in the *CYP2e1*+/+ mice injected with cisplatin. Of particular interest was the induction of the p21 in the *CYP2e1*−/− control mice with further up-regulation following administration of cisplatin. We postulate that the up-regulation of p21 in the control *CYP2e1*−/− mice could represent a compensatory mechanism that may be induced in response to the aberration or deletion of the *CYP2e1* gene. This additional up-regulation of p21 in cisplatin-treated *CYP2e1*−/− mice might further contribute in preventing the DNA damaged cells entering the cell cycle. Experimentally, overexpression of p21 in tumor-bearing animals may effectively inhibit the growth/proliferation of the malignant cells and could serve as an interesting animal model for cancer study and attractive target for future drug design.

CONCLUSION

Our results demonstrate a critical role of CYP2E1 in cisplatin-induced nephrotoxicity and initiation of apoptosis. It could stimulate the identification and localiza-

tion of specific CYP isozymes in the human renal tubular cells and the development of specific inhibitors that could prevent or ameliorate cisplatin-induced renal injury. A more thorough understanding of the renal stress response and its molecular interactions with the mitochondrial apoptotic pathway will certainly be important areas of research in the future.

ACKNOWLEDGMENTS

Reprint requests to Radhakrishna Baliga, M.D., Department of Pediatrics, Division of Nephrology, University of Mississippi Medical Center, 2500 North State Street, Jackson, MS 39216-4505.
E-mail: rbaliga@ped.umsmed.edu

REFERENCES

1. Lebwohl D, Canetta R: Clinical development of platinum complexes in cancer therapy: An historical perspective and an update. *Eur J Cancer* 34:1522–1534, 1998
2. Ries F, Klastersky J: Nephrotoxicity induced by cancer chemotherapy with special emphasis on cisplatin toxicity. *Am J Kidney Dis* 8:368–379, 1986
3. Safirstein R, Winston J, Goldstein M, *et al*: Cisplatin nephrotoxicity. *Am J Kidney Dis* 8:356–367, 1986
4. Baliga R, Zhang Z, Baliga M, *et al*: In vitro and in vivo evidence suggesting a role for iron in cisplatin-induced nephrotoxicity. *Kidney Int* 53:394–401, 1998
5. Davis CA, Nick HS, Agarwal A: Manganese superoxide dismutase attenuates cisplatin-induced renal injury: importance of superoxide. *J Am Soc Nephrol* 12:2683–2690, 2001
6. Lieberthal W, Triaca V, Levine J: Mechanisms of death induced by cisplatin in proximal tubular epithelial cells: apoptosis vs. necrosis. *Am J Physiol* 270 (4 Pt 2):F700–F708, 1996
7. Lau AH: Apoptosis induced by cisplatin nephrotoxic injury. *Kidney Int* 56:1295–1298, 1999
8. Gonzalez FJ: The molecular biology of cytochrome P450s. *Pharmacol Rev* 40:243–288, 1988
9. Kuthan H, Tsuji H, Graf H, Ullrich V: Generation of superoxide anion as a source of hydrogen peroxide in a reconstituted monooxygenase system. *FEBS Lett* 91:343–345, 1978
10. Nordblom GD, Coon MJ: Hydrogen peroxide formation and stoichiometry of hydroxylation reactions catalyzed by highly purified liver microsomal cytochrome P-450. *Arch Biochem Biophys* 180:343–347, 1977
11. Baliga R, Zhang Z, Baliga M, Shah SV: Evidence for cytochrome P-450 as a source of catalytic iron in myoglobinuric acute renal failure. *Kidney Int* 49:362–369, 1996
12. Baliga R, Zhang Z, Baliga M, *et al*: Role of cytochrome P-450 as a source of catalytic iron in cisplatin-induced nephrotoxicity. *Kidney Int* 54:1562–1569, 1998
13. Bysani GK, Kennedy TP, Ky N, *et al*: Role of cytochrome P-450 in reperfusion injury of the rabbit lung. *J Clin Invest* 86:1434–1441, 1990
14. Paller MS, Jacob HS: Cytochrome P-450 mediates tissue-damaging hydroxyl radical formation during reoxygenation of the kidney. *Proc Natl Acad Sci USA* 91:7002–7006, 1994
15. Liu H, Bigler SA, Henegar JR, Baliga R: Cytochrome P450 2B1 mediates oxidant injury in puromycin induced nephrotic syndrome. *Kidney Int* 62:868–876, 2002
16. Guengerich FP, Kim DH, Iwasaki M: Role of human cytochrome

17. Lucas D, Farez C, Bardou LG, Vaisse J, *et al*: Cytochrome P450 2E1 activity in diabetic and obese patients as assessed by chlorzoxazone hydroxylation. *Fundam Clin Pharmacol* 12:553–558, 1998
18. Mandl J, Banhegyi G, Kalapos MP, Garzo T: Increased oxidation and decreased conjugation of drugs in the liver caused by starvation. Altered metabolism of certain aromatic compounds and acetone. *Chem Biol Interact* 96:87–101, 1995
19. McCarver DG, Byun R, Hines RN, *et al*: A genetic polymorphism in the regulatory sequences of human CYP2E1: Association with increased chlorzoxazone hydroxylation in the presence of obesity and ethanol intake. *Toxicol Appl Pharmacol* 152:276–281, 1998
20. Dai Y, Rashba-Step J, Cederbaum AI: Stable expression of human cytochrome P4502E1 in HepG2 cells: Characterization of catalytic activities and production of reactive oxygen intermediates. *Biochemistry* 32:6928–6937, 1993
21. Ekstrom G, Ingelman-Sundberg M: Rat liver microsomal NADPH-supported oxidase activity and lipid peroxidation dependent on ethanol-inducible cytochrome P-450 (P-450IIE1). *Biochem Pharmacol* 38:1313–1319, 1989
22. Lee SS, Buters JT, Pineau T, *et al*: Role of CYP2E1 in the hepatotoxicity of acetaminophen. *J Biol Chem* 271:12063–12067, 1996
23. el-Deiry WS, Tokino T, Velculescu VE, *et al*: WAF1, a potential mediator of p53 tumor suppression. *Cell* 75:817–825, 1993
24. Gutteridge JM, Rowley DA, Halliwell B: Superoxide-dependent formation of hydroxyl radicals in the presence of iron salts. *Biochem J* 199:263–265, 1981
25. Gutteridge JM, Rowley DA, Halliwell B: Superoxide-dependent formation by hydroxyl radicals and lipid peroxidation in the presence of iron salts. *Biochem J* 206:605–609, 1982
26. Ueda N, Baliga R, Shah SV: Role of "catalytic" iron in an animal model of minimal change nephrotic syndrome. *Kidney Int* 49:370–373, 1996
27. Kutty RK, Nagineni CN, Kutty G, *et al*: Increased expression of heme oxygenase-1 in human retinal pigment epithelial cells by transforming growth factor-beta. *J Cell Physiol* 159:371–378, 1994
28. Trakshel GM, Kutty RK, Maines MD: Purification and characterization of the major constitutive form of testicular heme oxygenase. The noninducible isoform. *J Biol Chem* 261:11131–11137, 1986
29. Bradd SJ, Dunn MJ: Analysis of membrane proteins by Western blotting and enhanced chemiluminescence. *Methods Mol Biol* 19:211–218, 1993
30. Hsu SM, Raine L, Fanger H: A comparative study of the peroxidase-antiperoxidase method and an avidin-biotin complex method for studying polypeptide hormones with radioimmunoassay antibodies. *Am J Clin Pathol* 75:734–738, 1981
31. Gartel AL, Ye X, Goufman E, *et al*: Myc represses the p21(WAF1/CIP1) promoter and interacts with Sp1/Sp3. *Proc Natl Acad Sci USA* 98:4510–4515, 2001
32. Zhang JG, Lindup WE: Cisplatin-induced changes in adenine nucleotides in rat kidney slices: amelioration by tiopronin and procaine. *J Pharm Pharmacol* 49:1136–1140, 1997
33. Rosenkranz AR, Schmaldienst S, Stuhlmeier KM, *et al*: A microplate assay for the detection of oxidative products using 2′,7′-dichlorofluorescin-diacetate. *J Immunol Methods* 156:39–45, 1992
34. Baliga R, Zhang Z, Shah SV: Role of cytochrome P-450 in hydrogen peroxide-induced cytotoxicity to LLC-PK1 cells. *Kidney Int* 50:1118–1124, 1996
35. Ramachandra S, Studzinski GP: Morphological and biochemical criteria of apoptosis, in *Cell Growth and Apoptosis*, edited by Studzinski GP, New York, Oxford University Press, 1995, pp 119–141
36. Dennery PA: Regulation and role of heme oxygenase in oxidative injury. *Curr Top Cell Regul* 36:181–199, 2000
37. Hirt DL, Jacobson HR: Functional effects of cytochrome P450 arachidonate metabolites in the kidney. *Semin Nephrol* 11:148–155, 1991
38. Carroll MA, Balazy M, Huang DD, *et al*: Cytochrome P450-derived renal HETEs: Storage and release. *Kidney Int* 51:1696–1702, 1997

P-450 IIE1 in the oxidation of many low molecular weight cancer suspects. *Chem Res Toxicol* 4:168–179, 1991

39. BALIGA R, UEDA N, WALKER PD, SHAH SV: Oxidant mechanisms in toxic acute renal failure. *Am J Kidney Dis* 29:465–477, 1997

40. LIU H, BALIGA M, BALIGA R: Effect of cytochrome P450 2E1 inhibitors on cisplatin-induced cytotoxicity to renal proximal tubular epithelial cells. *Anticancer Res* 22:863–868, 2002

41. NATH KA, BALLA G, VERCELLOTTI GM, *et al*: Induction of heme oxygenase is a rapid, protective response in rhabdomyolysis in the rat. *J Clin Invest* 90:267–270, 1992

42. AGARWAL A, BALLA J, ALAM J, *et al*: Induction of heme oxygenase in toxic renal injury: A protective role in cisplatin nephrotoxicity in the rat. *Kidney Int* 48:1298–1307, 1995

43. SHIRAISHI F, CURTIS LM, TRUONG L, *et al*: Heme oxygenase-1 gene ablation or expression modulates cisplatin-induced renal tubular apoptosis. *Am J Physiol* 278:F726–F736, 2000

44. INGUAGGIATO P, GONZALEZ-MICHACA L, CROATT AJ, *et al*: Cellular overexpression of heme oxygenase-1 up-regulates p21 and confers resistance to apoptosis. *Kidney Int* 60:2181–2191, 2001

45. BISSELL DM, HAMMAKER LE: Cytochrome P-450 heme and the regulation of hepatic heme oxygenase activity. *Arch Biochem Biophys* 176:91–102, 1976

46. UEDA N, KAUSHAL GP, SHAH SV: Apoptotic mechanisms in acute renal failure. *Am J Med* 108:403–415, 2000

47. KLUCK RM, BOSSY-WETZEL E, GREEN DR, NEWMEYER DD: The release of cytochrome c from mitochondria: A primary site for Bcl-2 regulation of apoptosis. *Science* 275:1132–1136, 1997

48. REED JC: Cytochrome c: Can't live with it—Can't live without it. *Cell* 91:559–562, 1997

49. TAKEDA M, KOBAYASHI M, SHIRATO I, *et al*: Cisplatin-induced apoptosis of immortalized mouse proximal tubule cells is mediated by interleukin-1 beta converting enzyme (ICE) family of proteases but inhibited by overexpression of Bcl-2. *Arch Toxicol* 71:612–621, 1997

50. LI P, NIJHAWAN D, BUDIHARDJO I, *et al*: Cytochrome c and dATP-dependent formation of Apaf-1/caspase-9 complex initiates an apoptotic protease cascade. *Cell* 91:479–489, 1997

51. FINKEL T: Oxygen radicals and signaling. *Curr Opin Cell Biol* 10:248–253, 1998

52. RASHBA-STEP J, CEDERBAUM AI: Generation of reactive oxygen intermediates by human liver microsomes in the presence of NADPH or NADH. *Mol Pharmacol* 45:150–157, 1994

53. BONDY SC, NADERI S: Contribution of hepatic cytochrome P450 systems to the generation of reactive oxygen species. *Biochem Pharmacol* 48:155–159, 1994

54. LABAER J, GARRETT MD, STEVENSON LF, *et al*: New functional activities for the p21 family of CDK inhibitors. *Genes Dev* 11:847–862, 1997

55. HARPER JW, ADAMI GR, WEI N, *et al*: The p21 Cdk-interacting protein Cip1 is a potent inhibitor of G_1 cyclin-dependent kinases. *Cell* 75:805–816, 1993

56. MEGYESI J, SAFIRSTEIN RL, PRICE PM: Induction of p21WAF1/CIP1/SDI1 in kidney tubule cells affects the course of cisplatin-induced acute renal failure. *J Clin Invest* 101:777–782, 1998